Organic Electronics 13 (2012) 2312–2318

Contents lists available at SciVerse ScienceDirect

Organic Electronics

journal homepage: www.elsevier.com/locate/orgel

Infrared proximity sensor using organic light-emitting diode with quantum dots converter

En-Chen Chen [a], Han-Cheng Yeh [b], Yu-Chiang Chao [c], Hsin-Fei Meng [c,*], Hsiao-Wen Zan [b], Yun-Chi Liang [d], Chin-Ping Huang [e], Teng-Ming Chen [d,*], Chih-Feng Wang [f], Chu-Chen Chueh [f], Wen-Chang Chen [f,*], Sheng-Fu Horng [a]

[a] Department of Electrical Engineering, National Tsing Hua University, Hsinchu 300, Taiwan, ROC
[b] Department of Photonics and the Institute of Electro-Optical Engineering, National Chiao Tung University, Hsinchu 300, Taiwan, ROC
[c] Institute of Physics, National Chiao Tung University, Hsinchu 300, Taiwan, ROC
[d] Department of Applied Chemistry, National Chiao Tung University, Hsinchu 300, Taiwan, ROC
[e] Nanotechnology Research Center, Nano-Instrumentation and Application Division, Industrial Technology Research Institute, Hsinchu 310, Taiwan, ROC
[f] Department of Chemical Engineering and Institute of Polymer Science and Engineering, National Taiwan University, Taipei 10617, Taiwan, ROC

ARTICLE INFO

Article history:
Received 2 February 2012
Received in revised form 12 April 2012
Accepted 13 May 2012
Available online 20 June 2012

Keywords:
Quantum dots
PLED
Infrared proximity sensor

ABSTRACT

An efficient visible-to-infrared conversion film is made by blending CdTe quantum dots (CdTe QDs) of 12 nm diameter in a polyvinylpyrrolidone 360 (PVP 360) polymer matrix cast by water solution. The solid-state photoluminescence quantum efficiency exceeds 10% with emission peak at 810 nm. Strong 810 emission is obtained by combining the quantum dot film and a green polyfluorene light-emitting diode. Color filter is used to remove residual light below 780 nm to make it entirely invisible. Infrared photo-detector is made by blending poly[5-(5-(2,5-bis(decyloxy)-4-methylphenyl)thiophen-2-yl)-2,3-bis(4-(2-ethylhexyloxy)phenyl)-7-(5-methylthiophen-2-yl)thieno[3,4-b]pyrazine] (PBDOTTP) with band-gap 1.2 eV and (6,6)-phenyl-C61-butyric acid methyl ester (PCBM). The pixel contains one PD surrounded by four PLED on its four sides. The active areas of the five devices are all 1 cm by 1 cm and they are on the same plane. Infrared proximity sensor with photo-current over 300 nA at 10 cm object distance is achieved by detecting the reflected infrared signal.

1. Introduction

Infrared emission and detection based on III–V inorganic semiconductor has been widely used for object proximity sensor. Recently there is a high interest to develop large-area sensor array in thin and light-weight flexible substrate for robot artificial skin and other forms of flexible electronics [1–3]. It is therefore desirable to have large-area planar infrared light source and detector. The wavelength needs to exceed 780 nm such that the sensor array is invisible to human and can operate in the background. Longer wavelength also has the advantage of lower loss due to scattering. Despite of the strong infrared emission inorganic semiconductor light-emitting diodes (LED) are individually encapsulated devices and cannot be made as a large film. Organic LED can give large-area planar emission but only for the visible light [4–9]. In order to realize the large-area thin-film proximity and distance sensor array using infrared signal a visible-to-infrared conversion film must be developed in combination with visible organic LED. Inorganic phosphor is successful in conversion of blue emission from inorganic LED to longer wavelength in the visible range [10–14]. However phosphor with efficient conversion to infrared does not exist. Infrared organic laser dyes is known to have poor photoluminescence in solid film. Some conjugated polymers have low band-gap in the near infrared red, mostly developed for solar cells. They however have poor photoluminescence efficiency as the repeat unit usually has a donor–acceptor pair resulting in displaced

* Corresponding authors. Address: Institute of Physics, National Chiao Tung University, Hsinchu 300, Taiwan, ROC (H.-F. Meng).
E-mail addresses: meng@mail.nctu.edu.tw (H.-F. Meng), tmchen@mail.nctu.edu.tw (T.-M. Chen), chenwc@ntu.edu.tw (W.-C. Chen).

1566-1199/$ - see front matter © 2012 Elsevier B.V. All rights reserved.
http://dx.doi.org/10.1016/j.orgel.2012.05.010

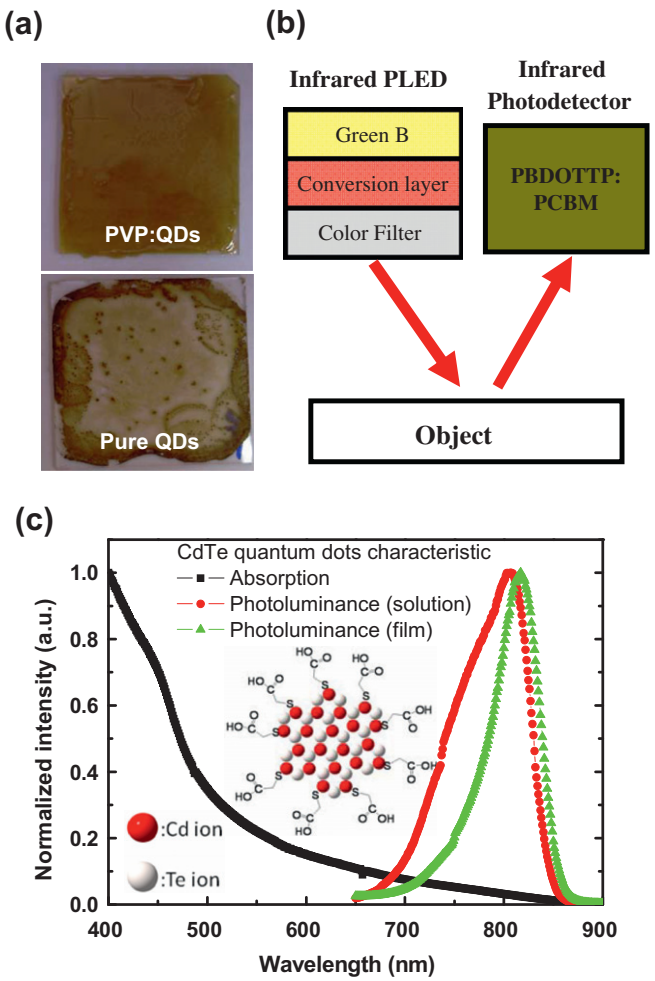

Fig. 1. (a) The images of conversion film made by pure QDs and blend solution of QDs and PVP 360. (b) The schematic working principle of proximity sensor. (c) The absorption and PL spectra (solution and film) of the CdTe QDs. The inset shows the chemical structure of QDs.

conduction and valence band wave functions and low optical transition matrix element.

Quantum dots (QDs) made of II–VI and III–V compounds have high photoluminescence quantum efficiency in solution and cover a wide spectral range from violet to near infrared by tuning chemical composition and dot size [15]. For example CdTe quantum dots (CdTe QDs) has emission from 550 nm to 850 nm depending on the particle size which is comparable to the exciton Bohr radius of a few nanometers. QDs functionalized by organic surfactants have been employed in fluorescent labeling for biological research [16–18]. They are also incorporated in the active layers of semiconductor devices including solar cell and LED but the efficiency is not so high [19–22]. Despite of the challenges in the active-layer applications, it turns out that QDs satisfies the requirements for the desired external conversion film as they have strong infrared photoluminescence, form large-area film by solution deposition, and has broad absorption spectrum for easy excitation by organic LED. The only uncertainty is whether the strong photoluminescence in solution can be translated into solid film. In solution the QDs are surrounded by the surfactants which have high affinity to the solvent on one end. Once the solvent is evaporated the surfactant may no longer cover the QDs surface and self-quenching of luminescence may occur.

In this work we develop a water-soluble CdTe QDs, capped with 3-mercaptoproproionic acid, through microwave-assisted synthesis. The QDs has strong near infrared emission peaked at 810 nm in both water solution and film. Surprisingly the solid-state self-quenching effect of the CdTe QDs is small, suggesting either the surfactants remain on the dot surface or the dot emission is not compromised as they are in direct contact. Uniform film can be formed by blending the CdTe QDs with a polymer matrix as shown in Fig. 1(a). Strong planar infrared emission is obtained by combining the QDs conversion film and a green polymer LED. For photo-detector we synthesize a low band-gap conjugated polymer with absorption up to 1000 nm. Highly sensitive planar proximity sensor is achieved by detecting the reflected signal from a nearby object by the photo-detector using a blend of the low

band-gap polymer and fullerene derivative. The difference between this work and our previous one [1] is also further stressed. In our previous work using laser dye the emission is slightly visible to human eyes while using quantum dot in this work the emission wavelength of 810 nm is entirely beyond the human vision. Besides, high voltage of −20 V is required for the photo-detector using P3HT as the semiconductor, whereas only −3 V is required using the low bandgap polymer PBDOTTP in this work. The schematic working principle of proximity sensor is shown in Fig. 1(b). The entire proximity sensor is planar and the operation is completely invisible to human eyes.

2. Experimental

The polymer light-emitting diode (PLED) and photo-detector (PD) are fabricated on glass substrates with a poly-(3,4-ethylenedioxythiophene): poly-(styrenesulfonate) (PEDOT:PSS) layer on a patterned indium-tin-oxide layer. The PEDOT:PSS film is baked at 200 °C for 15 min in an ambient environment. On the top of the PEDOT:PSS surface, the polymer LED structure is cross-linkable TFB (23 nm)/Green B (70 nm)/Ca (35 nm)/Al (100 nm). The hole transport layer of cross-linkable poly[(9,9-dioctylfluorenyl-2,7-diyl)-co-(4,4″-{N-[4-secybutylphenyl]}diphenylamine)] (cross-linkable TFB) (0.5 wt.% in toluene) is formed by spin coating and then baked at 180 °C for 60 min. The emitting layer is also formed by spin coating polyfluorene derivative LUMATION Green B by Dow Chemical (1.2 wt.% in toluene) and then baking at 130 °C for 30 min.

The active layer of the near infrared PD is the blend of poly[5-(5-(2,5-bis(decyloxy)-4-methylphenyl)thiophen-2-yl)-2,3-bis(4-(2-ethylhexyloxy)phenyl)-7-(5-methylthiophen-2-yl)thieno[3,4-b]pyrazine] (PBDOTTP) and (6,6)-phenyl-C61-butyric acid methyl ester (PCBM) where PBDOTTP is the electron donor and PCBM is the acceptor. The photo-detector has photo-current response from 400 nm to 1000 nm wavelength. PBDOTTP: PCBM (1:1 wt.%) solution in 1,2-dichlorobenzene is spin coated at 450 rpm upon PEDOT:PSS to form a 100 nm film. The PD is completed by coating Ca (35 nm)/Al (100 nm) cathode. All devices are processed and packaged in a glove box.

The synthesis of PBDOTTP is described below: 322 mg of 2,2′-(2,5-bis(decyloxy)-1,4-phenylene)bis(4,4,5,5-tetramethyl-1,3,2-dioxaborolane) (0.5 mmol), 434 mg of 5,7-bis(5-bromothiophen-2-yl)-2,3-bis4-(2-ethylhexyloxy)phenyl)thieno[3,4-b]pyrazine (0.5 mmol), and 15 ml toluene were used to afford 425 mg dark blue solid (78.5%). ^{1}H-NMR (CD_2Cl_2, δ ppm): 7.58 (br, 10H), 6.87 (br, 4H), 4.08 (br, 4H), 3.95 (br, 4H), 1.24–1.94 (br, 50H), 0.82–0.97 (br, 18H). Molecular weight (estimated from GPC): 9890, PDI = 1.62. Calcd. for $(C_{68}H_{90}N_2O_4S_3)_n$: C, 74.54; H, 8.28; N, 2.56; S, 8.78. Found: C, 73.54; H, 8.26; N, 2.33; S, 8.70 [23,24].

The synthesis of CdTe QDs is described below: 0.2 mol of $Cd(NO_3)_2$ 4H2O solution, 0.34 mol of MPA solution were mixed in a 30 ml solution, and the pH of the solution was adjusted to 11.5 by drop-wise addition of 25% NH_4OH solution with stirring until the mixture solution turn to colorless. Under stirring, Na_2TeO_3 (0.05 M, 1 ml) was added through a syringe into the Cd precursor solution. In order to reduce Na_2TeO_3 solution, NaBH4 (0.0625 g) was added into above solution. A series of high-quality CdTe NCs were prepared under microwave irradiation located by program process. Sodium tellurite (99%) and Cadmium nitrate tetrahydrate (98%) were purchased from Aldrich. 3-Mercaptopropionic acid (MPA) (98%) was purchased from Fluka. NaBH4 (99%) was obtained from Shanghai Chemical Reagents Company. All chemicals were used without additional purification. All solutions were prepared using Milli-Q water (Millipore) as the solvent. The synthesis of the QDs is to be described elsewhere [22,25].

Photoluminescence and photoluminescence excitation spectra were acquired using a Spex Fluorolog-3 fluorimeter (Jobin Yvon Instrument S.A. Inc.). Photoluminescence quantum efficiency (PL quantum efficiency) were measured using indocyanine green (ICG) standards (95% in ethanol and 13% in DMSO). Optical densities (OD) of QD and dye standard solutions were measured using a U-3010 UV–Vis spectrophotometer (Hitachi) and the PL quantum efficiency were obtained by Eq. (1):

$$QY_{QD} = QY_{dye}\frac{I_{QD}}{I_{dye}}\frac{OD_{dye}}{OD_{QD}}\frac{n_{QD}^2}{n_{dye}^2} \quad (1)$$

Where $n_{QD,dye}$ is the refractive index and $I_{QD,dye}$ is the integrated fluorescence signal for the QD and dye solutions, respectively[26].

3. Results and discussions

Using one-pot microwave irradiation reduction route synthesize CdTe QDs, which emit at near-infrared range (∼810 nm) and diameter around 12 nm, are fast and simply. The composition of CdTe QDs are Cd, Te ions and 3-mercaptopropionic acid (MPA) as passivated and stabilizer. The chemical structure of the surfactant is shown in Fig. 1(c). The MPA supported the thio group with Cd ion (from CdTe QDs) to form the covalent bonding and carboxylic acid to stabilize the QDs in water environment. The photoluminescence (PL) of the QDs in water solution is shown in Fig. 1(c) with peak at 810 nm, longer than the limit of human vision of 780 nm. The absolute PL quantum efficiency in solution is measured to be 15%. The CdTe QDs, has broad absorption spectrum range (<800 nm), could be excited by organic LED. Solid film of CdTe QDs can be formed by drop casting on glass substrate. For pure QDs the film is not uniform as cracks form during the drying process as shown in Fig. 1(a). Despite of the poor uniformity strong PL comes out from the pure film upon excitation, suggesting low self-quenching. To improve the film uniformity the QDs are blended in a polymer matrix of polyvinylpyrrolidone 360 (PVP 360) with QDs to polymer weight ratio of 1:10 and drop cast in water solution. The film is annealed at 100 °C for 20 min to remove water, resulting a solid film of 500 μm thick. The thickness is so chosen to ensure a nearly complete absorption of the exciting green light. Good uniformity for the conversion film is achieved as shown in Fig. 1(a).

The device characteristics of the Green B polymer LED is shown in Fig. 2(a). One advantage of Green B is its high

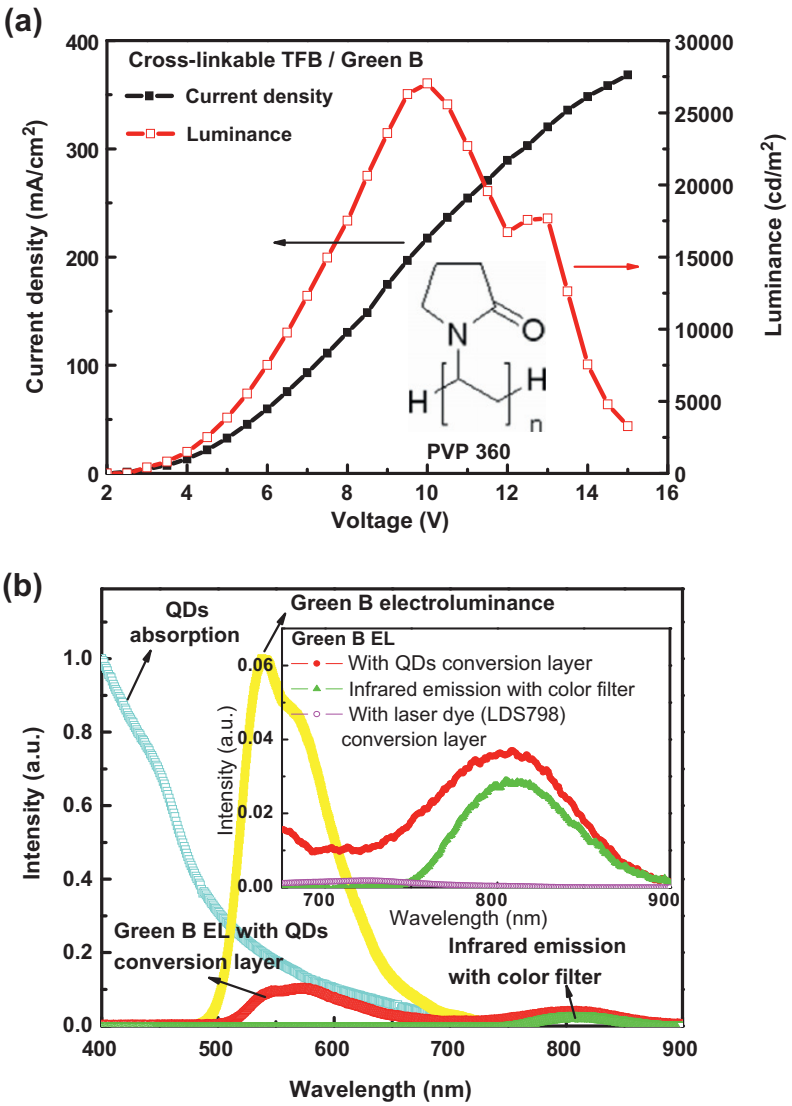

Fig. 2. (a) The current density and luminance of the green PLED. (b) The EL spectrum of Green B (yellow line) is converted to near infrared emission (green line) by QDs conversion layer and color filter. The inset shows the enlarged spectrum from 675 nm to 900 nm and the comparison of photoluminescence (PL) intensity in solid-state host between CdTe quantum dots and organic laser dye (LDS798). (For interpretation of the references to colour in this figure legend, the reader is referred to the web version of this article.)

luminance. The green emission of the polymer LED is externally converted into invisible infrared emission by the conversion layer made of QDs blended in PVP 360 matrix. The spectral intensity of the original green emission and the converted infrared emission are shown in Fig. 2(b). The green emission around 550 nm is greatly reduced by the QDs absorption, and emission around 810 nm due to QDs PL results. Note 550 nm is at the broad absorption tail of the QDs, therefore thick film is necessary for nearly complete absorption. The solid-state PL quantum efficiency of the conversion film can be estimated as the ratio between the area of the infrared spectral band and the area of the reduced excitation spectral band which is the area between the yellow and red curves in Fig. 2(b). The result is 10%, which is about 2/3 of the solution PL quantum efficiency of 15% for QDs. Considering the inevitable loss due to reflection and scattering this estimate indicates that there is only small, if any, effect of self-quenching. Because the blend contains a high concentration of QDs in weight, the dots must be in contact with each other in general. The possible origins of quenching PL quantum efficiency include trapping of electrons at the surface of the QDs by PVP and chemical induction of defects on the surface of QDs as a result of interactions between surface atoms and PVP molecules [27]. The persistence of the luminescence in solid film suggests that either the QDs are still well covered by the surfactant in the solid state, or the electronic structure of the excited state is not affected by the direct contact and wavefunction overlap. Solid-state PL efficiency over 10% for QDs is in sharp contrast to

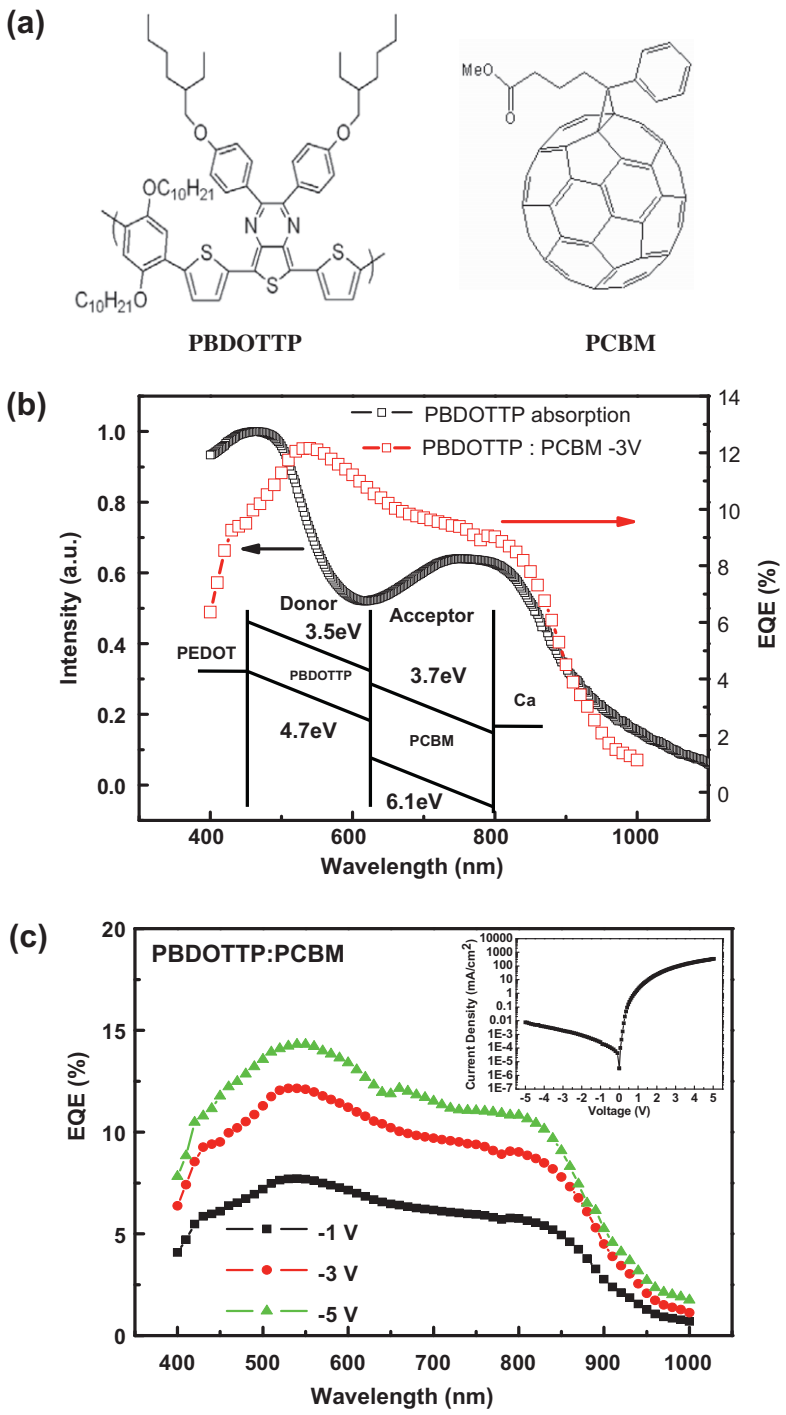

Fig. 3. (a) The chemical structures of PBDOTTP and PCBM. (b) The absorption spectra of pure PBDOTTP film and the EQE of PBDOTTP:PCBM bulk heterojunction photo-detector under reverse bias of 3 V. (c) The EQE of the near infrared photo-detector at various reverse bias. The inset shows the *J–V* characteristic in the dark of device.

infrared organic laser dye whose PL efficiency is below 1% no matter in solution or in film [28]. The direct comparison in solid-state host between CdTe quantum dots and organic laser dye (LDS798) shows in inset of Fig. 2(b). In addition to high PL efficiency, our QDs films show great stability. The luminescence does not show considerable decay two months after drop cast. The QDs conversion film alone does not give completely invisible emission because of the small residual green emission as shown in red in Fig. 2(b). In addition, the long wavelength tail of the Green B emission extends beyond 700 nm and is not absorbed by the QDs. The tail is however within the human vision boundary of

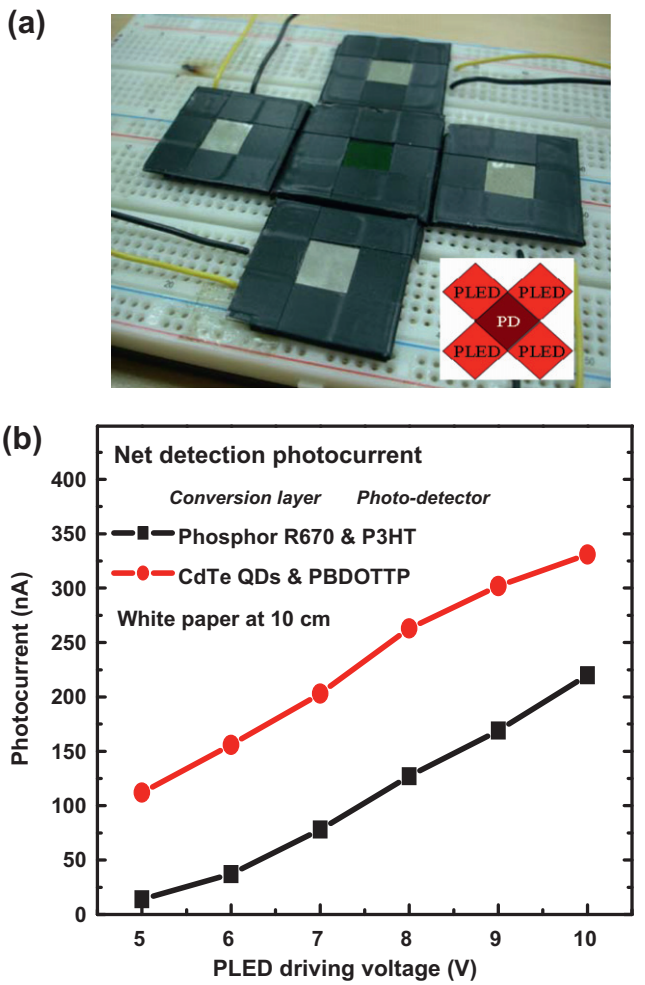

Fig. 4. (a) The pixel contains one PD surrounded by four PLED on its four sides. The active areas of the five devices are all 1 cm by 1 cm. The cross-talks are avoided by sealing the substrates of PLED and PD by black tapes except or the active area. (b) The net detection signal of one pixel proximity sensor under static condition, comparable to our previous work [30]. (For interpretation of the references to colour in this figure legend, the reader is referred to the web version of this article.)

780 nm. An absorptive color filer (HWB780 from Apisc) which removes photons with wavelength shorter than 780 nm is added to the conversion film, the resulting spectrum is shown in Fig. 2(b) as the green curve. 700 nm to 900 nm range is shown in detail in the inset. HWB 780 filter only slightly reduce the 810 nm PL of the QDs but completely removes the visible part of the spectrum.

Both the polymer LED and the conversion film are solution processed. Even though they are on glass substrate in this work, in the future they can be made on large-area and potentially flexible substrate. In order to have the sensor array as a flexible thin film, the infrared photo-detector is also made of polymers. Low band-gap polymer PBDOTTP shown in Fig. 3(a) is synthesized. The polymer has a low band-gap of 1.2 eV, with lowest unoccupied molecular orbital (LUMO) of 3.5 eV below vacuum and highest occupied molecular orbital (HOMO) of 4.7 eV below vacuum as shown in Fig. 3(b). PBDOTTP is blended with electron acceptor PCBM with 1:1 weight ratio to form the active layer of the photo-detector. Excitons created in PBDOTTP by photon absorption are dissociated at the interface with PCBM and form charge carriers. The electron is collected by the Ca electrode and hole collected by the PEDOT electrode under reverse bias as shown in Fig. 3(b). The active layer thickness is only 100 nm and smaller than the absorption depth because the limited solubility of PBDOTTP makes it difficult to deposit thicker films. In principle higher photo-current will result if thicker film is used. The external quantum efficiency (EQE) of the photo-detector, defined as number of electron per absorbed photon, is shown in Fig. 3(b) as a function of wavelength. The film absorption spectrum of PBDOTTP is also shown for comparison. The low band-gap of PBDOTTP allows photocurrent generation up to 1000 nm. EQE is about 10% at the QDs emission peak of 810 nm under reverse bias of 3 V [29], and the Fig. 3(c) shows the EQE of photo-detector at various reverse bias. The *J*–*V* characteristic in the dark of device is shown in inset of Fig. 3(c).

The characteristics of a single proximity sensor under static voltage condition are shown in Fig. 4. The pixel

contains one photo-detectors (PD) surrounded by four polymer LED (PLED) on its four sides. The active areas of the five devices are all 1 cm by 1 cm and they are on the same plane. The cross-talks are avoided by sealing the substrates of PLED and PD by black tapes except or the active area. This ensures that the PLED light does not enter PD directly without reflection by the object. The pixel of proximity sensor is shown in Fig. 4(a). A white paper as the object is placed in parallel to the plane. The off current −4.24 μA is defined as the PD current when the PLED is off, it is the summation of the PD dark current and the photo-current due to the background indoor lighting. The net detection photo-current is the difference between the PD currents at PLED on state and at PLED off state. The only origin of the net photo-current is the light emitted by the PLED and reflected by the white paper. Net photo-current as a function of PLED voltage at fixed paper distance of 10 cm is shown in Fig. 4(b). We successfully increase the net detection photo-current, comparable to our previous work [30]. The significant enhancement is also shown in Fig. 4(b). At 5 V PLED voltage the photo-current is already over 100 nA. Such higher signal can be easily resolved by signal processing circuits [30]. At 9 V, the photo-current reaches 300 nA and sensitivity up to 15 cm is realized.

4. Conclusion

Infrared object proximity sensor is achieved by converting the visible emission of a polymer LED by a layer of inorganic QDs blended in a polymer matrix. The conversion from green to infrared around 810 nm has a high quantum efficiency due to the lack of self-quenching of functionalized QDs. The infrared signal is reflected by an object and detected by a polymer photo-detector using a low band-gap conjugated polymer. Proximity sensing with high sensitivity up to 15 cm is realized and the operation is entire invisible to human eyes. Because the polymer LED, the QDs film, and the polymer photo-detector are all made by solution process, a thin light-weight large-area sensor array can be realized by integrating all the components on a potentially flexible substrate. Such thin sensor array can be used, for example, as the artificial skin for robots in intimate interaction with human beings.

Acknowledgments

This work is supported by the National Science Council of Taiwan under Contract No. NSC99-2628-M-009-001 and No. NSC98-2113-M-009-005-MY3. HFM thanks R. Yen and G. Walze at Bayer for fruitful discussions.

References

[1] E.C. Chen, S.R. Tseng, J.H. Ju, C.M. Yang, H.F. Meng, S.F. Horng, C.F. Shu, Appl. Phys. Lett. 93 (2008) 063304.
[2] V.J. Lumelsky, M.S. Shur, S. Wagner, IEEE Sens. J. 1 (2001) 41.
[3] R.H. Reuss et al., IEEE Proceedings 93 (2005) 7.
[4] S.H. Yang, C.S. Hsu, J. Polym. Sci., Polym. Chem. 47 (2009) 2713.
[5] C.D. Muler, A. Falcou, N. Reckefuss, M. Rojahn, V. Wiederhirn, P. Rudati, H. Frohne, O. Nuyken, H. Becker, K. Meerholz, Nature 421 (2003) 829.
[6] J. Yu, J. Wang, S. Lou, T. Wang, Y. Jiang, Displays 29 (2008) 493.
[7] S.R. Forrest, Nature 428 (2004) 911.
[8] Q.F. Xu, J.Y. Ouyang, Y. Yang, T. Ito, J. Kido, Appl. Phys. Lett. 83 (2003) 4695.
[9] X. Gong, S. Wang, D. Moses, G.C. Bazan, A.J. Heeger, Adv. Mater. 17 (2005) 2053.
[10] L. Zhou, J. Wei, F. Gong, J. Huang, L. Yi, Solid State Chem. 1337 (2008) 181.
[11] K.M. Lee, K.M. Cheah, B.L. An, M.L. Gong, Y.L. Liu, Appl. Phys. A 80 (2005) 337.
[12] N.J. Xiang, L.M. Leung, S.K. So, J. Wang, Q. Su, M.L. Gong, Mater. Lett. 60 (2006) 2909.
[13] H. Iwanaga, A. Amano, F. Aiga, K. Harada, M.J. Oguchi, J. Alloys Compd. 408 (2006) 921.
[14] H. Yan, H. Wang, P. He, J. Shi, M. Gong, Synth. Met. 161 (2011) 748.
[15] U.R. Genger, M. Grabolle, S.C. Jaricot, R. Nitschke, T. Nann, Nat. Methods 5 (2008) 763.
[16] D.M. Willard, A.V. Orden, Nat. Mater. 2 (2003) 575.
[17] P.M.A. Farias, A. Fontes, A. Galembeck, R.C.B.Q. Figueiredo, B.S. Santos, J. Braz. Chem. Soc. 19 (2008) 352.
[18] C.P. Huang, Y.K. Li, T.M. Chen, Biosens. Bioelectron. 22 (2007) 1835.
[19] H.J. Lee, D.Y. Kim, J.S. Yoo, J. Bang, S. Kim, S.M. Park, Bull. Korean Chem. Soc. 28 (2007) 953.
[20] Y.L. Lee, B.M. Huang, H.T. Chien, Chem. Mater. 20 (2008) 6903.
[21] M.A. Schreuder, K. Xiao, I.N. Ivanov, S.M. Weiss, S.J. Rosenthal, Nano Lett. 10 (2010) 573.
[22] A. Shavel, N. Gaponik, A. Eychmüller, J. Phys. Chem. B 110 (2006) 19280.
[23] C.L. Liu, J.H. Tsai, W.Y. Lee, W.C. Chen, S.A. Jenekhe, Macromolecules 41 (2008) 6952.
[24] C.C. Chueh, M.H. Lai, J.H. Tsai, C.F. Wang, W.C. Chen, J. Polym. Sci. Part A: Polym. Chem. 48 (2010) 74.
[25] T. Pons, N. Lequeux, B. Mahler, S. Sasnouski, A. Fragola, B. Dubertret, Chem. Mater. 21 (2009) 1418.
[26] Y. He, H.T. Lu, L.M. Sai, W.Y. Lai, Q.L. Fan, L.H. Wang, W. Huang, J. Phys. Chem. B 110 (2006) 13370.
[27] V. Biju, R. Kanemoto, Y. Matsumoto, S. Ishii, S. Nakanishi, T. Itoh, Y. Baba, M. Ishikawa, J. Phys. Chem. C 111 (2007) 7924.
[28] P. Sarkar, R. Luchowski, S. Raut, N. Sabnis, A. Remaley, A.G. Lacko, S. Thamake, Z. Gryczynski, I. Gryczynski, Biophys. Chem. 153 (2010) 61.
[29] E.C. Chen, S.R. Tseng, Y.C. Chao, H.F. Meng, C.F. Wang, W.C. Chen, C.S. Hsu, S.F. Horng, Synthetic Met. 161 (2011) 1618.
[30] E.C. Chen, C.Y. Shih, M.Z. Dai, H.C. Yeh, Y.C. Chao, H.F. Meng, H.W. Zan, W.R. Liu, Y.C. Chiu, Y.T. Yeh, C.J. Sun, S.F. Horng, C.S. Hsu, IEEE T. Electron Dev. 58 (2011) 1215.